FEMS MICROBIOLOGY ECOLOGY

RESEARCH ARTICLE

Field-scale labelling and activity quantification of methane-oxidizing bacteria in a landfill-cover soil

Ruth Henneberger[1], Eleonora Chiri[1], Jan Blees[2], Helge Niemann[2], Moritz F. Lehmann[2] & Martin H. Schroth[1]

[1]Institute of Biogeochemistry and Pollutant Dynamics, ETH Zurich, Zurich, Switzerland; and [2]Department of Environmental Sciences, University of Basel, Basel, Switzerland

Correspondence: Martin H. Schroth, Institute of Biogeochemistry and Pollutant Dynamics, ETH Zurich, Universitätstr. 16, CH-8092 Zurich, Switzerland. Tel.: +41 44 6336039; fax: +41 44 6331122; e-mail: martin.schroth@env.ethz.ch

Received 7 June 2012; revised 15 August 2012; accepted 18 August 2012.
Final version published online 19 September 2012.

DOI: 10.1111/j.1574-6941.2012.01477.x

Editor: Tillmann Lueders

Keywords
gas push-pull test; stable isotope probing; phospholipid ester-linked fatty acids; methanotrophs; *in situ* labelling.

Abstract

Aerobic methane-oxidizing bacteria (MOB) play an important role in soils, mitigating emissions of the greenhouse gas methane (CH_4) to the atmosphere. Here, we combined stable isotope probing on MOB-specific phospholipid fatty acids (PLFA-SIP) with field-based gas push-pull tests (GPPTs). This novel approach (SIP-GPPT) was tested in a landfill-cover soil at four locations with different MOB activity. Potential oxidation rates derived from regular- and SIP-GPPTs agreed well and ranged from 0.2 to 52.8 mmol CH_4 (L soil air)$^{-1}$ day^{-1}. PLFA profiles of soil extracts mainly contained C_{14} to C_{18} fatty acids (FAs), with a dominance of C_{16} FAs. Uptake of ^{13}C into MOB biomass during SIP-GPPTs was clearly indicated by increased $\delta^{13}C$ values (up to *c.* 1500‰) of MOB-characteristic FAs. In addition, ^{13}C incorporation increased with CH_4 oxidation rates. In general, FAs $C_{14:0}$, $C_{16:1\omega8}$, $C_{16:1\omega7}$ and $C_{16:1\omega6}$ (type I MOB) showed highest ^{13}C incorporation, while substantial ^{13}C incorporation into FAs $C_{18:1\omega8}$ and $C_{18:1\omega7}$ (type II MOB) was only observed at high-activity locations. Our findings demonstrate the applicability of the SIP-GPPT approach for *in situ* quantification of potential CH_4 oxidation rates and simultaneous labelling of active MOB, suggesting a dominance of type I MOB over type II MOB in the CH_4-oxidizing community in this landfill-cover soil.

Introduction

Methane (CH_4) is a potent greenhouse gas contributing strongly to global warming (Denman *et al.*, 2007). Aerobic methane-oxidizing bacteria (MOB) use CH_4 as the sole source of carbon and energy, thereby reducing CH_4 flux from various methanogenic environments to the atmosphere, for example, from wetlands, rice paddies and anoxic sediments. In addition, cover soils of CH_4-producing, municipal-waste landfills often harbour highly diverse and active MOB communities (Chen *et al.*, 2007; Gebert *et al.*, 2009; Kumaresan *et al.*, 2009; Henneberger *et al.*, 2012). Based on the current understanding, most MOB can be placed either within the phylum *Proteobacteria* or the phylum *Verrucomicrobia* (Murrell, 2010). The latter MOB are a recently discovered group of thermo-acidophilic methane-oxidizing *Verrucomicrobia* (see review by Op den Camp *et al.*, 2009), but they are yet to be taxonomically validated. The methane-oxidizing members of the *Proteobacteria* comprise two major groups: type I and type II MOB, belonging to *Gammaproteobacteria* and *Alphaproteobacteria*, respectively. The two groups differ not only in their phylogenetic affiliation, but also with respect to their biochemical and physiological properties, such as carbon assimilation pathway and cellular membrane structure (Hanson & Hanson, 1996; Murrell, 2010).

Because these microorganisms are significant modulators of global CH_4 emissions, MOB diversity, abundance and activity for various environments have been studied to great extent under laboratory conditions and in natural settings. Such studies generally focus on the *pmoA* gene, which encodes a subunit of the particulate methane monooxygenase (pMMO), a key enzyme in the aerobic CH_4 oxidation pathway (Hanson & Hanson, 1996). Moreover, the phylogeny of the *pmoA* gene correlates well with the 16S rRNA gene (Kolb *et al.*, 2003). In addition to *pmoA*-based phylogeny, the proteobacterial MOB can also be differentiated to a certain degree based on the chemical

composition of their cellular membranes, for instance the distribution of phospholipid ester-linked fatty acids (PLFA). Fatty acid (FA) profiles of type I MOB membranes are generally dominated by C_{14} and C_{16} FAs, while type II MOB membranes contain a larger portion of C_{18} FAs (Bowman *et al.*, 1991; Hanson & Hanson, 1996; Niemann *et al.*, 2006). In particular, the C_{16} FA $C_{16:1\omega5t}$ is considered to be characteristic for type I MOB, while the C_{18} FAs $C_{18:1\omega8c}$, $C_{18:2\omega7c,12c}$ and $C_{18:2\omega6c,12c}$ are characteristic for type II MOBs (Bowman *et al.*, 1991; Hanson & Hanson, 1996; Bowman, 2006; Bodelier *et al.*, 2009). Distinctive PLFA profiles of different groups can be exploited to link MOB function with community structure by following the incorporation of isotopic tracers (e.g. ^{13}C) into the biomass (i.e. into FAs) of active MOB. In fact, the first reported application of PLFA stable isotope probing (SIP) was the use of ^{13}C-labelled CH_4 to identify active MOB (Boschker *et al.*, 1998).

Since then, SIP methodologies have evolved and are now widely applied to study active subpopulations of complex microbial communities (Neufeld *et al.*, 2007). For example, PLFA-SIP using $^{13}CH_4$ has been used to investigate active MOB in samples derived from various soil and sediment environments (Knief *et al.*, 2003; Chen *et al.*, 2008; Shrestha *et al.*, 2008). Such incubation experiments have provided valuable insights into ecological aspects of MOB communities, for example the influence of CH_4 availability (Knief *et al.*, 2006), nitrogen fertilization (Mohanty *et al.*, 2006) or flooding regimes (Bodelier *et al.*, 2012) on the structure and activity of MOB populations. However, reports on the application of this technique to landfill-cover soils are scarce (Crossman *et al.*, 2004). In addition, PLFA-SIP studies were generally performed under controlled laboratory conditions that may vary significantly from natural habitats, thus hindering direct extrapolation of the results back to the field.

Few studies have applied SIP directly in the field (Middleburg *et al.*, 2000; Padmanabhan *et al.*, 2003). For example, Pombo *et al.* (2002, 2005) used aqueous push-pull tests in combination with PLFA-SIP in a petroleum-contaminated aquifer to identify dominant nitrate- and sulphate-reducing bacteria while simultaneously determining their activity. Recently, the push-pull test technique was modified for gaseous substrates (Urmann *et al.*, 2005). During such a gas push-pull test (GPPT), a mixture of reactive gases (e.g. CH_4 and O_2) and nonreactive tracer gases (e.g. Ar, Ne or He) is injected into the soil at a location of interest. After injection, the gas flow is reversed and the soil-air-diluted gas mixture is extracted from the same location and sampled periodically. Reaction rate constants can subsequently be derived from differences in the breakthrough curves of the reactant and a suitable tracer gas (Urmann *et al.*, 2008; Gómez *et al.*, 2009). GPPTs have been applied successfully to quantify CH_4 oxidation in a variety of pristine and anthropogenically influenced environments, such as peat bog, the vadose zone above a contaminated methanogenic aquifer or a landfill-cover soil (Urmann *et al.*, 2007, 2008; Gómez *et al.*, 2009; Henneberger *et al.*, 2012). Nevertheless, the combination of the GPPT technique with PLFA-SIP has not been attempted for a field-based study.

The aim of the present work was to develop an efficient methodology that enables labelling of active MOB at the field scale while simultaneously quantifying *in situ* CH_4 oxidation rates. The novel approach presented here combines $^{13}CH_4$ PLFA-SIP with the GPPT technique. We applied this method to the cover soil of a Swiss landfill and tested its applicability at four locations with differences in CH_4 oxidation activity.

Material and methods

Study site

All sampling and field-based studies were performed at the Lindenstock landfill (Liestal, BL, Switzerland), which has been described in detail elsewhere (Henneberger *et al.*, 2012; Schroth *et al.*, 2012). Experiments were carried out in August and September 2011 at five locations that are in close proximity to locations C1, EM and NM, previously described and characterized for their MOB diversity and activity (Henneberger *et al.*, 2012). During summer 2010, these locations exhibited differences in CH_4 oxidation rates with the highest apparent first-order rate constant (k; for details on calculations see below) measured at C1 (4.69 h^{-1}), followed by EM (0.52 h^{-1}) and NM (0.16 h^{-1}). We termed the locations for the present study C1-1, C1-2, C1-3, EM-1 and NM-1 according to their proximity to the previously described locations (within *c.* 100–250 cm).

Soil properties

Soil temperature was recorded throughout the study period at 50 cm depth in 3-h intervals, using Thermochron iButton dataloggers (DS1921G#F50; Maxim, Sunnyvale, CA) that were installed near locations C1 and NM. Volumetric water content was determined by time-domain reflectometry (TDR100; Campbell Scientific, Loughborough, UK), using brass-rod pairs (15 mm o.d., 70 cm long) previously installed close to locations C1, EM and NM.

Borehole installation and soil sample collection

Soil cores were collected using a HUMAX hollow-stem auger system (80 mm i.d.; Martin Burch AG, Rothenburg,

Switzerland). At each location, we drilled to a depth of *c.* 55 cm, and soil core samples were collected in plastic sleeves from 45 to 55 cm depth. For subsequent GPPTs, Teflon tubes (2 mm i.d.) were inserted into the borehole to reach down to 50 cm depth. The tubes were protected from particulate clogging by covering the tips with steel wool, and the lower end of the tube was embedded in *c.* 10 cm of sand (45–55 cm depth; 0.7–1.2 mm Quartz sand; Carlo Bernasconi AG, Zürich, Switzerland). The borehole was subsequently backfilled with a 1 : 1 mixture of sand and commercially available Bentonite (Fatto, Migros, Switzerland), followed by a final 5 cm of Bentonite to ground level. The exposed ends of the tubes were fitted with three-way valves. Location C1-3, which served as reference, was backfilled as described above, but without installation of a Teflon tube.

Approximately 24 h after performing GPPTs with $^{13}CH_4$ (hereafter referred to as SIP-GPPT), an area of *c.* 50 × 50 cm was excavated to a depth of 45 cm. The sand in the final 10 cm of the borehole was removed, and soil material for further analyses was collected from 45 to 55 cm depth along the rim of the bore hole using sterile tools.

All soil samples collected during initial drilling and excavation after SIP-GPPTs were homogenized and subsampled immediately on site with sterile spatulas and transferred to sterile aluminium foil. Samples were stored on ice for several hours and frozen at -20 °C upon return to the laboratory.

Gas push-pull tests

The GPPTs performed at locations C1-1, C1-2, EM-1 and NM-1 were slightly modified from recently described methods (Urmann *et al.*, 2005; Gómez *et al.*, 2009; Henneberger *et al.*, 2012). Regular GPPTs were performed 5–6 days after installation of the tubes, using *c.* 20 L of gas mixture containing 2 vol.% CH_4, 18 vol.% O_2 and 26.7 vol.% each of helium (He), neon (Ne) and argon (Ar). The gas mixture was injected into the soil at 50 cm depth over a period of 30 min at a flow rate of *c.* 0.63 L min^{-1}. Following injection, the gas flow was reversed and the gas mixture diluted with soil air was extracted from the same location for 30 min at *c.* 0.58 L min^{-1} flow rate (corresponding to a total volume of *c.* 17 L). For gas concentration analysis, two soil-air background samples were collected prior to injection, three samples of the gas mixture were collected during injection (at 10-min intervals), and during extraction, samples were taken every 2 min. All gas samples were collected in 20-mL glass vials (sealed with butyl rubber septa and metal crimp caps) after flushing the vials with at least 500 mL of the respective gas using an inflow and an outflow needle. During extraction, gas exiting the outflow needle was vented into the atmosphere.

SIP-GPPTs were performed 2–3 weeks after tube installation at locations C1-1, EM-1 and NM-1, using *c.* 21–22 L of gas mixture containing 5 vol.% $^{13}CH_4$, 20 vol.% O_2 and 25 vol.% each of He, Ne and Ar. At location C1-2, the following gas mixture was used: 2 vol.% $^{13}CH_4$, 18 vol.% O_2 and 26.7 vol.% each of He, Ne and Ar. Gas samples were collected during the injection and extraction phase in similar fashion as before. However, gas exiting the vials' outflow needle during extraction was collected in the original gas-bag and, upon completion of each SIP-GPPT, re-injected slowly into the soil over a period of *c.* 100–105 min to allow further oxidation of $^{13}CH_4$ and therefore additional ^{13}C incorporation after completion of the GPPT.

For regular and SIP-GPPTs, kinetic parameters of CH_4 oxidation (apparent first-order rate constants *k*, potential CH_4 oxidation rates) were estimated from extraction data using a simplified method as previously described (Schroth & Istok, 2006; Urmann *et al.*, 2008; Gómez *et al.*, 2009). Briefly, for each extracted sample, the natural logarithm of the relative concentration (extracted concentration divided by injected concentration, corrected for natural background) of CH_4 divided by the relative concentration of a tracer (here Ar) is plotted against the gas mixture's residence time in the soil. The negative slope of the linear regression was taken as apparent first-order rate constant *k*, characterizing indigenous CH_4 oxidation for variable CH_4-limited conditions. Thus, these *k* values represent averages over the entire data set assuming first-order kinetics. For direct comparison of activity, potential oxidation rates were subsequently calculated for a CH_4 concentration of 0.5 vol.% (a concentration observed in extracted samples of most GPPTs). Values of *k* used in these calculations were determined from a subset of samples near 0.5 vol.% CH_4 to more accurately describe the reaction kinetics at that concentration.

Fatty acid extraction and preparation of derivates

The extraction procedure and preparation of fatty acid methyl esters (FAME) was carried out according to previously described methods (Elvert *et al.*, 2003; Niemann *et al.*, 2005). Briefly, total lipid extracts were obtained from *c.* 20 g of wet soil by subsequent ultrasonication with organic solvents of decreasing polarity [dichloromethane/methanol (1 : 2, v/v), dichloromethane/methanol (2 : 1, v / v), dichloromethane]. An internal standard (FA *n*-$C_{19:0}$) with known concentration and $\delta^{13}C$ value was added to the soil sample prior to extraction. FA glycerol esters constituting glycolipids and phospholipids were cleaved by saponifi-

cation with methanolic KOH solution. FAs were methylated with methanolic BF_3 solution yielding FAMEs. Double-bond positions of monounsaturated FAs were determined by the analysis of dimethyl disulphide adducts (Nichols *et al.*, 1986; Moss & Lambertfair, 1989).

Analysis of gas samples

Samples collected during GPPTs were analysed by gas chromatography (GC) using a Thermo Scientific TRACE GC Ultra gas chromatograph. Gas contents for Ar, Ne, He and O_2 were separated over a PLOT Molsieve 5A column (50 m × 0.53 mm i.d., 50 μm df; held isothermally at 30 °C; Varian, Palo Alto, CA), using H_2 as carrier gas (22 mL min^{-1}), and quantified with a thermal conductivity detector. Methane was separated over a packed steel column (2 m long, 1/16″ o.d., 1 mm i.d.; packed with Porapak N 100/120 mesh) using N_2 as carrier gas (3.2 mL min^{-1}) and quantified by flame ionization detection (FID).

Analysis of fatty acids

FAs were identified, quantified and analysed for their stable carbon isotope composition using GC quadrupole mass spectrometry (GC-MS), GC-FID and GC-isotope-ratio mass spectrometry (GC-IRMS), respectively. GC was performed using a Thermo Scientific TRACE GC Ultra gas chromatograph equipped with a split/splitless injector and a 60-m apolar DB-5 ms fused silica column (0.25 mm i.d., 0.25 μm df). FAMEs were injected in splitless mode at 300 °C using He as a carrier gas at a constant flow rate of 1.2 mL min^{-1}. The initial oven temperature was set to 50 °C for 2 min, increased to 150 °C (10 °C min^{-1}) and finally raised to 300 °C at a rate of 4 °C min^{-1} with a final hold time of 30 min. Mass spectra of single lipid compounds were acquired using a Thermo Scientific DSQ II quadrupole mass spectrometer operated in electrospray ionization mode. The resulting mass spectra were compared to standard compounds and published data for identification. Compound-specific stable carbon isotope ratio measurements were performed using a Thermo Scientific DELTA V IRMS. Isotope ratios are given in the δ-notation (against Vienna Pee Dee Belemnite (VPDB)]. The FA $\delta^{13}C$ values were corrected for the introduction of additional carbon atoms during derivatization. The internal standard was used to monitor precision and reproducibility during measurements. Reported $\delta^{13}C$ values have an analytical precision of ± 1‰.

Results

MOB activity

MOB activity at locations C1-1, C1-2, EM-1 and NM-1 was assessed through regular GPPTs, using 2 vol.% nonlabelled CH_4 in the injected gas mixture. Logarithmic rate plots were reasonably linear over the entire data sets, indicating apparent first-order kinetics of the CH_4 oxidation reaction (representative rate plots of two locations shown in Supporting Information, Fig. S1). Deduced k values ranged from 0.10 h^{-1} at location NM-1 to 8.43 h^{-1} at location C1-1 (Table 1). Moreover, C1-1 and C1-2 showed the highest potential CH_4 oxidation rates (activity at 0.5 vol.% CH_4) with 46.0 and 55.7 mmol CH_4 (L soil air)$^{-1}$ day^{-1}, respectively, while considerably lower rates were observed at EM-1 [9.9 mmol CH_4 (L soil air)$^{-1}$ day^{-1}] and NM-1 [0.7 mmol CH_4 (L soil air)$^{-1}$ day^{-1}; Table 1].

SIP-GPPTs were performed with 5 vol.% $^{13}CH_4$ within 2–3 weeks after tube installation. Breakthrough curves and logarithmic rate plots were similar to those observed during regular GPPTs (representative breakthrough curves of two locations shown in Fig. 1; rate plots in Fig. S1),

Table 1. Activity of MOB in the Lindenstock landfill-cover soil determined at four different locations, using 2 vol.% CH_4 (regular GPPT) or 5 vol.% $^{13}CH_4$ (SIP-GPPT). In addition, absolute ^{13}C incorporation into C_{14} + C_{16} FAs (dominating type I MOB PLFA profiles) and C_{18} FAs (dominating type II MOB PLFA profiles) is shown

	MOB activity, regular GPPT		MOB activity, SIP-GPPT		^{13}C incorporation	
Location ID	First-order rate constants k ± SD (h^{-1})	Potential CH_4 oxidation rate ± SD [mmol CH_4 (L soil air)$^{-1}$ day^{-1}]	First-order rate constants k ± SD (h^{-1})	Potential CH_4 oxidation rate ± SD [mmol CH_4 (L soil air)$^{-1}$ day^{-1}]	C_{14} + C_{16}	C_{18}
					ng ^{13}C (μg extracts FA)$^{-1}$	
C1-1	8.43 ± 0.48	46.0 ± 6.0	6.10 ± 0.19	31.9 ± 2.8	0.304	0.013
C1-2	8.40 ± 0.25	55.7 ± 6.6	8.97 ± 0.48*	52.8 ± 5.6*	0.046	0.008
EM-1	1.46 ± 0.12	9.9 ± 1.0	0.96 ± 0.10	11.0†	0.029	0.008
NM-1	0.10 ± 0.01	0.7 ± 0.2	0.03 ± 0.01	0.2†	0.027	0.001

*SIP-GPPT done with 2 vol.% CH_4.

†Values estimated by extrapolating experimental data.

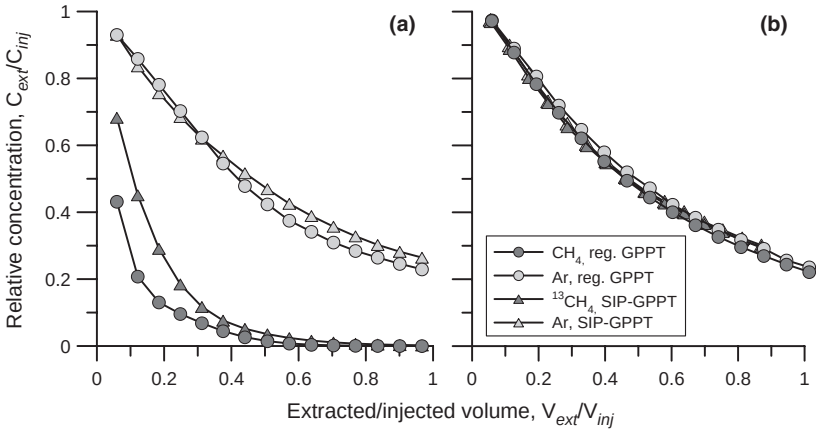

Fig. 1. Representative breakthrough curves of $CH_4/^{13}CH_4$ (dark grey symbols) and Ar (light grey symbols) observed during GPPTs at locations C1-1 (a) and NM-1 (b): circles symbolizing regular GPPTs with 2 vol.% CH_4 injection concentration, and triangles symbolizing SIP-GPPTs with 5 vol.% $^{13}CH_4$ injection concentration.

and resulting k values ranged from 0.03 h^{-1} at location NM-1 to 6.10 h^{-1} at location C1-1 (Table 1). Based on the high CH_4 oxidation rate determined from regular GPPT at location C1-2, only 2 vol.% $^{13}CH_4$ was applied during SIP-GPPT at this location, and the resulting k value was 8.97 h^{-1}. Potential CH_4 oxidation rates were 31.9 and 52.8 mmol CH_4 (L soil air)$^{-1}$ day^{-1} for C1-1 and C1-2, respectively. For locations EM-1 and NM-1, MOB activity was too low to reach concentrations of around 0.5 vol.% CH_4 during the extraction phase under the prevailing test conditions (5 vol.% $^{13}CH_4$ injection concentration). Potential oxidation rates therefore were estimated by extrapolating the experimental data, and values were similar to those observed during regular GPPTs (Table 1; Schroth *et al.*, 2012).

Methane concentrations measured in the soil-air background samples were low during the study period and comparable between the different locations, ranging from 4×10^{-4} vol.% (C1-2 and EM-1) to 9×10^{-4} vol.% (C1-1) during regular GPPTs and from 9×10^{-4} vol.% (EM-1) to 44×10^{-4} vol.% (NM-1) during SIP-GPPTs. During the time period activity measurements were carried out, soil temperatures at 50 cm depths were 18.5–19 °C (near location C1) and 17–17.5 °C (near location NM-1). The average volumetric water content of the 0- to 70-cm depth interval close to C1 showed only slight variations (0.24–0.26), and this value was constantly around 0.40 close to EM-1. Volumetric water content close to NM-1 varied from 0.35 at the date of tube installation to 0.19 at the date of final sample collection. Therefore, conditions varied only slightly throughout the study period and were similar to those observed during the 2010 campaign (Henneberger *et al.*, 2012).

Fatty acid composition

All sample extracts analysed contained substantial amounts of FAs, typically in the range of C_{14} to C_{18} (representative example of a partial GC-MS chromatogram shown in Fig. S2). The fractional abundance of selected FAs (C_{14}–C_{18}) at the reference location C1-3 (Fig. 2) and high-activity locations C1-1 and C1-2 (Fig. 3a and b) showed some similarities. Six dominant FAs ($C_{16:1\omega7}$, $C_{16:1\omega5}$, $C_{16:0}$, $C_{18:1\omega9}$, $C_{18:1\omega7}$ and $C_{18:0}$) were identified in all samples from these locations, with $C_{16:1\omega5}$ and $C_{16:0}$ being the most abundant (13–23% of total C_{14}–C_{18} FAs). Relative abundance of the remaining 15 minor FAs detected in these samples was also similar. However, the C1-3 samples lacked any detectable contribution from FA $C_{18:1\omega8}$. FA composition of samples collected at the intermediate- and low-activity locations (EM-1 and NM-1) showed some differences to the

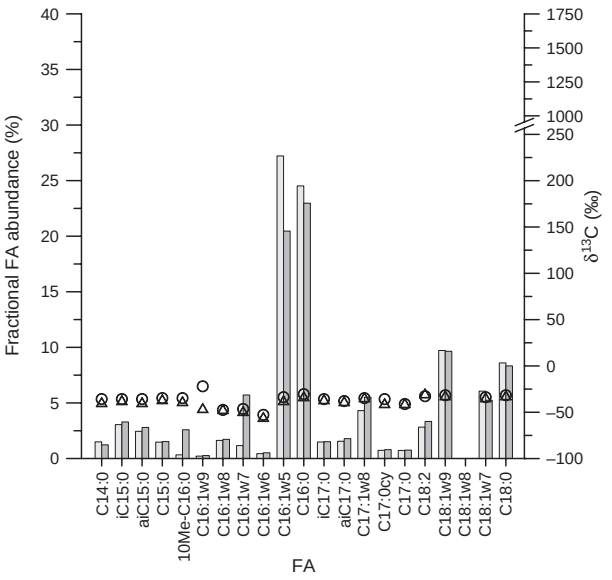

Fig. 2. Fractional abundance (left *y*-axis, bars) and $\delta^{13}C$ values (right *y*-axis, circles and triangles) of individual FAs extracted from reference location C1-3 at the beginning (light grey bars and circles) and end (dark grey bars and triangles) of the field study.

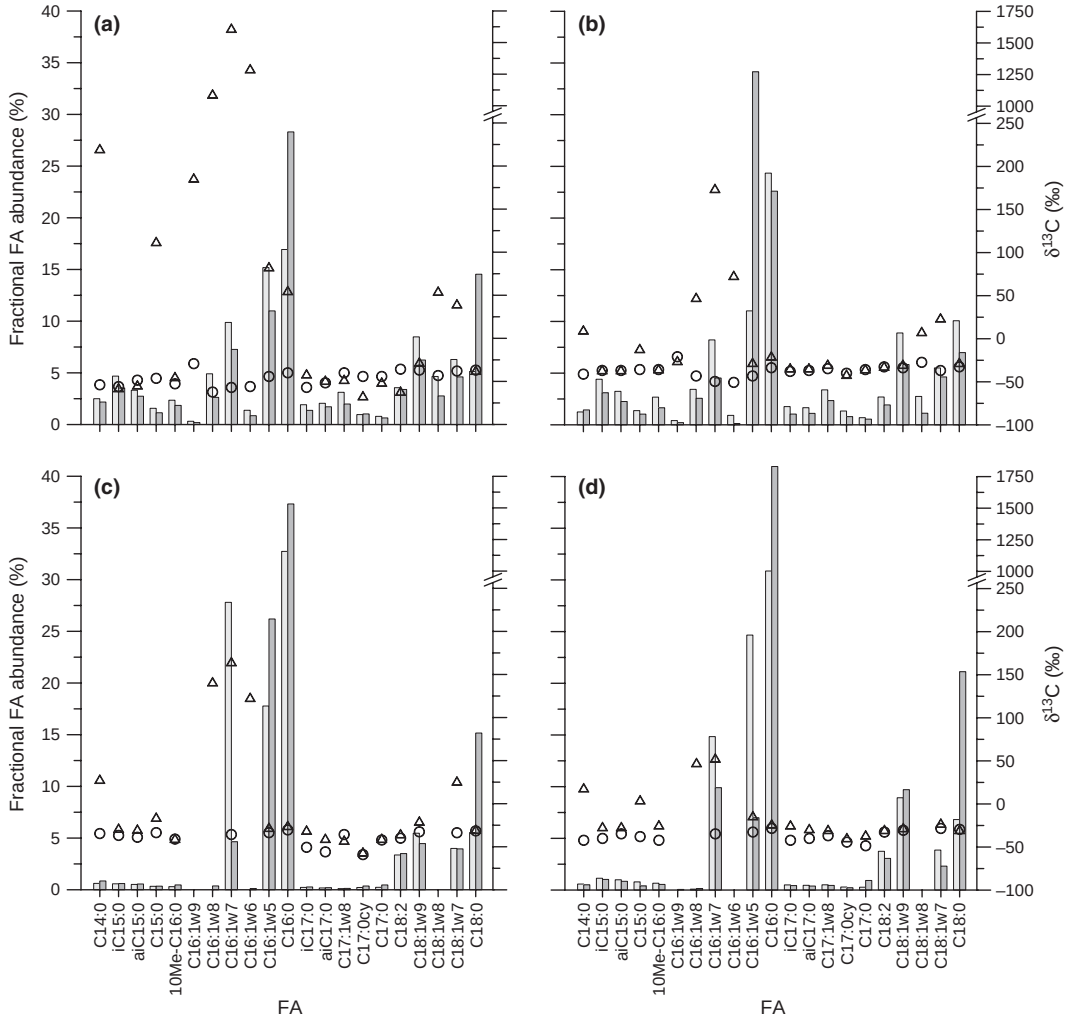

Fig. 3. Fractional abundance (left *y*-axis, bars) and $\delta^{13}C$ values (right *y*-axis, circles and triangles) of individual FAs extracted prior to regular GPPTs (light grey bars and circles) and after SIP-GPPTs (dark grey bars and triangles). (a) location C1-1, (b) location C1-2, (c) location EM-1, (d) location NM-1. For location C1-1 (a), $\delta^{13}C$ values are estimates due to GC-IRMS baseline shifts caused by extremely high $\delta^{13}C$ values.

high-activity locations. While a dominance of the FAs $C_{16:1\omega7}$, $C_{16:1\omega5}$, $C_{16:0}$, $C_{18:1\omega9}$ and $C_{18:0}$ was also observed in these sample extracts, their relative abundances differed from those detected at the high-activity locations (Fig. 3c and d). In addition, all other FAs in these samples were either present at very low concentrations, were detectable but could not be reliably quantified due to insufficient GC separation (in particular FAs $C_{16:1\omega8}$ and $C_{16:1\omega9}$), or were fully undetectable. Some differences in FA abundance were observed between samples taken at the same location before regular GPPTs and after SIP-GPPTs. These differences can be explained by substantial soil heterogeneity that was noticed at the different locations, in particular as sample collection after SIP-GPPTs was performed several cm away from the initial sampling point.

^{13}C labelling of fatty acids

The introduction of $^{13}CH_4$ during SIP-GPPTs led to the incorporation of ^{13}C into several FAs, as indicated by their increased $\delta^{13}C$ values relative to natural background values of -21‰ to -62‰ (as determined for FAs extracted from the reference location and all other locations prior to GPPTs; Figs 2 and 3). Incorporation of ^{13}C into biomass therefore appeared to increase with increasing MOB activity, as shown by higher $\delta^{13}C$ values detected at high-activity locations compared to low-activity locations (Fig. 3), and by increasing total ^{13}C incorporation (Table 1). The lower level of ^{13}C incorporation despite higher CH_4 oxidation activity observed for location C1-2 compared to C1-1 was likely caused by the lower

concentration of $^{13}CH_4$ applied during this SIP-GPPT (2 vs. 5 vol.% $^{13}CH_4$).

In addition to differences in the amount of ^{13}C incorporation observed, the varying levels of activity at the different locations seemed to be associated with differences in the FA labelling patterns. In general, at all locations, the most pronounced ^{13}C incorporation (i.e. highest $\delta^{13}C$ values) was found for the FAs $C_{14:0}$, $C_{15:0}$, $C_{16:1\omega8}$, $C_{16:1\omega7}$ and $C_{16:1\omega6}$. The high-activity locations (C1-1 and C1-2) and the intermediate-activity location (EM-1) also showed clear incorporation of ^{13}C into the FAs $C_{18:1\omega7}$ and $C_{18:1\omega8}$ (not detected at EM-1). This stands in contrast to observations made for the low-activity location NM-1, which displayed only a slight increase in $\delta^{13}C$ for FA $C_{18:1\omega7}$. In addition, at the two high-activity locations, ^{13}C label was recovered in the FAs $C_{16:1\omega5}$, $C_{16:0}$ (C1-1 and C1-2) and $C_{16:1\omega9}$ (C1-1 only), while these FAs were not labelled at the other two locations. At the reference location C1-3, where no GPPTs were performed, no enrichment in ^{13}C was detected, indicating the absence of natural fluctuations in $\delta^{13}C$ values throughout the study period (Fig. 2).

Injection of 5 vol.% $^{13}CH_4$ during the SIP-GPPT at the high-activity location C1-1 resulted in very high $\delta^{13}C$ values (> 1000‰) for the FAs $C_{16:1\omega8}$, $C_{16:1\omega7}$ and $C_{16:1\omega6}$. The high ^{13}C label content in these FAs had a biasing effect on the overall GC-IRMS performance, particularly for FAs with lower or no ^{13}C label content due to baseline shifting. Thus, while the results obtained here clearly provide evidence for high incorporation of CH_4-derived carbon, absolute $\delta^{13}C$ values obtained for C1-1 should be regarded with caution.

Discussion

Stable isotope probing of PLFA represents a widely used tool to identify active members within complex microbial assemblages, and this technique has been routinely used during laboratory experiments on MOB communities from various environments (Knief *et al.*, 2003; Chen *et al.*, 2008; Shrestha *et al.*, 2008). Here, we have successfully applied PLFA-SIP directly in the field using a modified GPPT approach. This combination of PLFA-SIP with GPPTs allowed the calculation of *in situ* CH_4 oxidation rates in parallel with isotope tracing of MOB through PLFA profile analysis. The SIP-GPPT was successfully implemented at several locations with differences in MOB activity and was shown to be applicable even at locations with relatively low CH_4 turnover rates. Methane oxidation rates at the Lindenstock landfill appeared to be stable over time, and rates observed here were comparable with those detected during previous studies (Gómez *et al.*, 2009; Henneberger *et al.*, 2012). Moreover, introduction of the ^{13}C label during SIP-GPPTs had no apparent effect on CH_4 oxidation rates.

SIP approaches are not limited to lipids, but also enable tracking of ^{13}C incorporation into DNA, RNA or proteins (Radajewski *et al.*, 2003; Jehmlich *et al.*, 2010). However, PLFA-SIP appears particularly suitable for field-based studies due to the low level of ^{13}C incorporation into FAs required for detection, the reliable extraction of FAs from soil samples and relatively simple processing of the extracted FAs (Neufeld *et al.*, 2007). It is important to mention that time is critical when gases are applied in the field, as rapid gas diffusion typically precludes long incubation times. Here, we demonstrated that a *c.* 3-h-long $^{13}CH_4$ incubation (GPPT and subsequent re-injection of gas mixture) was adequate for sufficient ^{13}C incorporation to be detectable by GC-IRMS within the FAs pool. In contrast, RNA-SIP and, in particular, DNA-SIP may require much longer incubation times up to days or weeks (Radajewski *et al.*, 2000; Noll *et al.*, 2008; Martineau *et al.*, 2010; Shrestha *et al.*, 2011). This is because unlike FAs, labelled nucleic acids need to be separated from their nonlabelled counterparts by density gradient centrifugation, requiring a larger label incorporation of at least 20 at.% compared to only 0.1 at.% ^{13}C for FAs (Boschker & Middleburg, 2002; Radajewski *et al.*, 2003).

On the other hand, phylogenetic resolution based on PLFA is lower compared to nucleic acids. To date, most PLFA-SIP studies on MOB communities are limited to distinguishing between type I and type II MOB. In addition, FAs currently considered to be characteristic for certain MOB might also be present in other, newly or yet to be described organisms. For example, FA $C_{16:1\omega8c}$ was long regarded as signature lipid for type I MOB, but was recently found to be contained in substantial amount in the type II MOB *Methylocystis heyeri* (Dedysh *et al.*, 2007). Nevertheless, in-depth studies on PLFA profiles of individual MOB strains, in particular novel isolates, may lead to the identification of novel signature lipids and may increase resolution in future PLFA-SIP studies on complex MOB communities. For example, Bodelier *et al.* (2009) detected novel and unusual $C_{18:2}$ FAs in PLFA profiles of several *Methylocystis* strains. They also demonstrated that a clear separation of type II MOB at the subgenus level is possible based on their characteristic PLFA profiles and that PLFA profiles of certain type I MOB cluster at the genus level.

In the landfill-cover soil analysed in this study, differences in PLFA profiles and ^{13}C incorporation into MOB signature FAs were observed between locations with contrasting CH_4 oxidation activity. Even though ^{13}C incorporation was only semi-quantitatively related to CH_4 oxidation rates, with higher levels of incorporation detected at locations with higher activity, it provided

valuable insights into the dominant, active MOB type at the different locations. In general, the most dominant ^{13}C incorporation was observed for FAs typically found in PLFA profiles characteristic for type I MOB. Labelling of FAs typically found in type II MOB was also clearly detected at most locations, but was far less pronounced, particularly at the lower-activity locations EM-1 and NM-1. In fact, the type II MOB-specific FA $C_{18:1\omega8}$ was not detected at these two locations, while type I MOB-characteristic FAs were dominant at all locations. These PLFA-based findings coincide with our previous analyses of the Lindenstock cover soil based on the *pmoA* gene, which also showed differences in MOB diversity and abundance between locations with different CH_4 oxidation activities (Henneberger *et al.*, 2012). Similar to the PLFA results, a general dominance of type I MOB-specific *pmoA* genes was detected in clone libraries and T-RFLP profiles. Type II MOB-specific *pmoA* genes comprised only a minor fraction of the T-RFLP profiles and were not detected in the clone library constructed from the low-activity location NM. These clear and consistent differences in type I and type II MOB communities at both the DNA and PLFA level suggest that the total (DNA-based study) and active (PLFA-SIP) MOB communities in the Lindenstock landfill-cover are indeed similar. Our results further suggest that CH_4 oxidation activity is mainly carried out by type I MOB and supported to a minor degree by type II MOB at locations with increased overall activity. These findings agree with a previous PLFA-SIP study on another loamy landfill-cover soil, where the dominance of type I MOB activity was also observed (Crossman *et al.*, 2004). Nevertheless, at all locations, high ^{13}C incorporation was observed for FAs with very low relative abundance, indicating that MOB comprise only a minor portion of the microbial community present at this site, particularly at the lower-activity locations.

The novel SIP-GPPT technique described here represents a promising advance for the labelling of active MOB directly in the field, hence minimizing procedural bias introduced during laboratory-based incubations. Substantial ^{13}C incorporation into type I and type II MOB signature FAs was observed despite short *in situ* incubation times, making this gas-phase approach feasible for field applications. Short incubation times most likely led to the lower levels of ^{13}C incorporation observed here in comparison with several laboratory-based studies on MOB communities (e.g. $\delta^{13}C$ of 6000‰ reported by Chen *et al.* (2008); Shrestha *et al.*, 2008). In this study, we attempted to compensate potentially low levels of ^{13}C incorporation due to short incubation times by increasing $^{13}CH_4$ injection concentrations (5 vol.% $^{13}CH_4$ during SIP-GPPTs compared to 2 vol.% CH_4 during regular GPPTs). However, our results indicate adequate ^{13}C incorporation into FAs even at low-activity locations, while suggesting that $^{13}CH_4$ concentration may be reduced for highly active locations to minimize overall bias during GC-IRMS analysis. In conclusion, the combination of PLFA-SIP with *in situ* CH_4 oxidation rate measurements employing GPPTs established a link between the structure and function of active MOB communities directly in a landfill-cover soil.

Acknowledgements

The authors would like to thank M. Vogt for help in the field. This work, as part of the European Science Foundation EUROCORES Program EuroEEFG, project MECOM-ECON, was supported from funds by the Swiss National Science Foundation (SNSF) under grant no. 31EE30-131170. Additional funding was provided by ETH Zurich.

References

Bodelier PL, Gillisen MJ, Hordijk K, Damste JS, Rijpstra WI, Geenevasen JA & Dunfield PF (2009) A reanalysis of phospholipid fatty acids as ecological biomarkers for methanotrophic bacteria. *ISME J* **3**: 606–617.

Bodelier PLE, Baer-Gilissen MJ, Meima-Franke M & Hordijk K (2012) Structural and functional response of methane-consuming microbial communities to different flooding regimes in riparian soils. *Ecol Evol* **2**: 106–127.

Boschker HTS & Middleburg JJ (2002) Stable isotopes and biomarkers in microbial ecology. *FEMS Microbiol Ecol* **40**: 85–95.

Boschker HTS, Nold SC, Wellsbury P, Bos D, de Graaf W, Pel R, Parkes RJ & Cappenberg TE (1998) Direct linking of microbial populations to specific biogeochemical processes by C-13-labelling of biomarkers. *Nature* **392**: 801–805.

Bowman JP (2006) The methanotrophs – the families Methylococcaceae and Methylocystaceae. *The Prokaryotes*, 3rd edn (Dworkin M, Falkow S, Rosenberg E, Schleifer K-H & Strackebrandt E, eds), pp. 266–289. Springer, New York, NY.

Bowman JP, Skerratt JH, Nichols PD & Sly LI (1991) Phospholipid fatty-acid and lipopolysaccharide fatty-acid signature lipids in methane-utilizing bacteria. *FEMS Microbiol Ecol* **85**: 15–22.

Chen Y, Dumont MG, Cebron A & Murrell C (2007) Identification of active methanotrophs in a landfill cover soil through detection of expression of 16S rRNA and functional genes. *Environ Microbiol* **9**: 2855–2869.

Chen Y, Dumont MG, McNamara NP, Chamberlain PM, Bodrossy L, Stralis-Pavese N & Murrell C (2008) Diversity of the active methanotrophic community in acidic peatland as assessed by mRNA and SIP-PLFA analyses. *Environ Microbiol* **10**: 446–459.

Crossman ZM, Abraham F & Evershed RP (2004) Stable isotope pulse-chasing and compound specific stable carbon

isotope analysis of phospholipid fatty acids to assess methane oxidizing bacterial populations in landfill cover soils. *Environ Sci Technol* **38**: 1359–1367.

Dedysh SN, Belova SE, Bodelier PLE, Smirnova KV, Khmelenina VH, Chidthaisong A, Trotsenko YA, Liesack W & Dunfield PF (2007) *Methylocystis heyeri* sp. nov., a novel type II methanotrophic bacterium possessing "signature" fatty acids of type I methanotrophs. *Int J Syst Evol Microbiol* **57**: 472–479.

Denman KL, Brasseur G, Chidthaisong A *et al.* (2007) Couplings between changes in the climate system and biogeochemistry. *Climate Change 2007: The Physical Science Basis. Contribution of Working Group I to the Fourth Assessment Report of the Intergovernmental Panel on Climate Change* (Solomon S, Qin D, Manning M, Chen Z, Marquis M, Averyt KB, Tignor M & Miller HL eds.), pp. 501–587. Cambridge University Press, Cambridge.

Elvert M, Boetius A, Knittel K & Jorgensen B (2003) Characterization of specific membrane fatty acids as chemotaxonomic markers for sulfate-reducing bacteria involved in anaerobic oxidation of methane. *Geomicrobiol J* **20**: 403–419.

Gebert J, Singh BK, Pan Y & Bodrossy L (2009) Activity and structure of methanotrophic communities in landfill cover soils. *Environ Microbiol Rep* **1**: 414–423.

Gómez KE, Gonzalez-Gil G, Lazzaro A & Schroth MH (2009) Quantifying methane oxidation in a landfill-cover soil by gas push-pull tests. *Waste Manag* **29**: 2518–2526.

Hanson RS & Hanson TE (1996) Methanotrophic bacteria. *Microbiol Rev* **60**: 439–471.

Henneberger R, Lüke C, Mosberger L & Schroth MH (2012) Structure and function of methanotrophic communities in a landfill-cover soil. *FEMS Microbiol Ecol* **81**: 52–65.

Jehmlich N, Schmidt F, Taubert M, Seifert J, Bastida F, von Bergen M, Richnow HH & Vogt C (2010) Protein-based stable isotope probing. *Nat Protoc* **5**: 1957–1966.

Knief C, Lipski A & Dunfield PF (2003) Diversity and activity of methanotrophic bacteria in different upland soils. *Appl Environ Microbiol* **69**: 6703–6714.

Knief C, Kolb S, Bodelier PLE, Lipski A & Dunfield PF (2006) The active methanotrophic community in hydromorphic soils changes in response to changing methane concentrations. *Environ Microbiol* **8**: 321–333.

Kolb S, Knief C, Stubner S & Conrad R (2003) Quantitative detection of methanotrophs in soil by novel *pmoA*-targeted real-time PCR assays. *Appl Environ Microbiol* **69**: 2423–2429.

Kumaresan D, Abell GCJ, Bodrossy L, Stralis-Pavese N & Murell C (2009) Spatial and temporal diversity of methanotrophs in a landfill cover soil are differentially related to soil abiotic factors. *Environ Microbiol Rep* **1**: 398–407.

Martineau C, Whyte LG & Greer CW (2010) Stable isotope probing analysis of the diversity and activity of methanotrophic bacteria in soils from the Canadian high arctic. *Appl Environ Microbiol* **76**: 5773–5784.

Middleburg JJ, Barraguet C, Boschker HTS, Herman PMJ, Moens T & Heip CHR (2000) The fate of intertidal microphytobenthos carbon: an *in situ* ^{13}C-labeling study. *Limnol Oceanogr* **45**: 1224–1234.

Mohanty SR, Bodelier PLE, Floris V & Conrad R (2006) Differential effects of nitrogenous fertilizers on methane-consuming microbes in rice field and forest soils. *Appl Environ Microbiol* **72**: 1346–1354.

Moss CW & Lambertfair MA (1989) Location of double-bonds in monounsaturated fatty-acids of *Campylobacter cryaerophila* with dimethyl disulfide derivatives and combined gas chromatography-mass spectrometry. *J Clin Microbiol* **27**: 1467–1470.

Murrell JC (2010) The aerobic methane oxidizing bacteria (Methanotrophs). *Handbook of Hydrocarbon and Lipid Microbiology* (Timmis KN, ed.), pp. 1953–1966. Springer, Berlin Heidelberg.

Neufeld JD, Dumont MG, Vohra J & Murrell JC (2007) Methodological considerations for the use of stable isotope probing in microbial ecology. *Microb Ecol* **53**: 435–442.

Nichols PD, Guckert JB & White DC (1986) Determination of monounsaturated fatty acid double-bond position and geometry for microbial monocultures and complex consortia by capillary GC-MS of their dimethyl disulphide adducts. *J Microbiol Meth* **5**: 49–55.

Niemann H, Elvert M, Hovland M *et al.* (2005) Methane emission and consumption at a North Sea gas seep (Tommeliten area). *Biogeosciences* **2**: 335–351.

Niemann H, Losekann T, de Beer D *et al.* (2006) Novel microbial communities of the Haakon Mosby mud volcano and their role as a methane sink. *Nature* **443**: 854–858.

Noll M, Frenzel P & Conrad R (2008) Selective stimulation of type I methanotrophs in a rice paddy soil by urea fertilization revealed by RNA-based stable-isotope probing. *FEMS Microbiol Ecol* **65**: 125–132.

Op den Camp HJM, Islam T, Stott MB, Harhangi HR, Hynes A, Schouten S, Jetten MSM, Birkeland NK, Pol A & Dunfield PF (2009) Environmental, genomic and taxonomic perspectives on methanotrophic Verrucomicrobia. *Environ Microbiol Rep* **1**: 293–306.

Padmanabhan P, Padmanabhan S, DeRito C, Gray A, Gannon D, Snape JR, Tsai CS, Park W, Jeon C & Madsen EL (2003) Respiration of ^{13}C-labeled substrates added to soil in the field and subsequent 16S rRNA gene analysis of ^{13}C-labeled soil DNA. *Appl Environ Microbiol* **69**: 1614–1622.

Pombo SA, Pelz O, Schroth MH & Zeyer J (2002) Field-scale C-labeling of phospholipid fatty acids (PLFA) and dissolved inorganic carbon: tracing acetate assimilation and mineralization in a petroleum hydrocarbon-contaminated aquifer. *FEMS Microbiol Ecol* **41**: 259–267.

Pombo SA, Kleikemper J, Schroth MH & Zeyer J (2005) Field-scale isotopic labeling of phospholipid fatty acids from acetate-degrading sulfate-reducing bacteria. *FEMS Microbiol Ecol* **51**: 197–207.

Radajewski S, Ineson P, Parekh NR & Murrell JC (2000) Stable-isotope probing as a tool in microbial ecology. *Nature* **403**: 646–649.

Radajewski S, McDonald IR & Murrell JC (2003) Stable-isotope probing of nucleic acids: a window to the function of uncultured microorganisms. *Curr Opin Biotechnol* **14**: 296–302.

Schroth MH & Istok JD (2006) Models to determine first-order rate coefficients form single-well push-pull tests. *Ground Water* **44**: 275–283.

Schroth MH, Eugster W, Gómez KE, Gonzalez-Gil G, Niklaus PA & Oester P (2012) Above- and below-ground methane fluxes and methanotrophic activity in a landfill-cover soil. *Waste Manage* **32**: 879–889.

Shrestha M, Abraham WR, Shrestha PM, Noll M & Conrad R (2008) Activity and composition of methanotrophic bacterial communities in planted rice soil studies by flux measurements, analyses of *pmoA* gene and stable isotope probing of phospholipid fatty acids. *Environ Microbiol* **10**: 400–412.

Shrestha M, Shrestha PM & Conrad R (2011) Bacterial and archaeal communities involved in the *in situ* degradation of ^{13}C-labelled straw in the rice rhizosphere. *Environ Microbiol Rep* **3**: 587–596.

Urmann K, Gonzalez-Gil G, Schroth MH, Hofer M & Zeyer J (2005) New field method: gas push-pull test for the in-situ quantification of microbial activities in the vadose zone. *Environ Sci Technol* **39**: 304–310.

Urmann K, Gonzalez-Gil G, Schroth MH & Zeyer J (2007) Quantification of microbial methane oxidation in an alpine peat bog. *Vadose Zone J* **6**: 705–712.

Urmann K, Schroth MH, Noll M, Gonzalez-Gil G & Zeyer J (2008) Assessment of microbial methane oxidation above a petroleum-contaminated aquifer using a combination of *in situ* techniques. *J Geophys Res* **113**: G02006. doi:10.1029/2006JG000363.

Supporting Information

Additional Supporting Information may be found in the online version of this article:

Fig. S1. Rate plots of CH_4 oxidation at locations C1-1 (dark grey symbols) and NM-1 (light grey symbols) during regular GPPT (circles) and SIP-GPPT (triangles).
Fig. S2. Representative example of partial GC-MS chromatogram of polar FAs in the range of C_{13} to C_{19}, extracted from location C1-1 after SIP-GPPT.

Please note: Wiley-Blackwell is not responsible for the content or functionality of any supporting materials supplied by the authors. Any queries (other than missing material) should be directed to the corresponding author for the article.